JAN 2

REPORT DOCUMENTATION PAGE	Form Approved OMB No. 0704-0188 JAN 25 2007

The public reporting burden for this collection of information is estimated to average 1 hour per response, including the time for reviewing instructions, searching existing data sources, gathering and maintaining the data needed, and completing and reviewing the collection of information. Send comments regarding this burden estimate or any other aspect of this collection of information, including suggestions for reducing the burden, to Department of Defense, Washington Headquarters Services, Directorate for Information Operations and Reports (0704-0188), 1215 Jefferson Davis Highway, Suite 1204, Arlington, VA 22202-4302. Respondents should be aware that notwithstanding any other provision of law, no person shall be subject to any penalty for failing to comply with a collection of information if it does not display a currently valid OMB control number.
PLEASE DO NOT RETURN YOUR FORM TO THE ABOVE ADDRESS.

1. REPORT DATE *(DD-MM-YYYY)*	2. REPORT TYPE	3. DATES COVERED *(From - To)*
25-01-2007	MAJOR REPORT	

4. TITLE AND SUBTITLE
ANATOMICAL AND PHYSIOLOGICAL CHRACTERISTICS OF THE FERRET LATERAL RECTUS MUSCLE AND ADBUCENS NUCLEUS

5a. CONTRACT NUMBER

5b. GRANT NUMBER

5c. PROGRAM ELEMENT NUMBER

6. AUTHOR(S)
MAJ BISHOP KEITH N
J. ROSS McCLUNG
STEPHEN J. GOLDBERG
MARY S. SHALL

5d. PROJECT NUMBER

5e. TASK NUMBER

5f. WORK UNIT NUMBER

7. PERFORMING ORGANIZATION NAME(S) AND ADDRESS(ES)
VIRGINIA COMMONWEALTH UNIV MED COL OF VA

8. PERFORMING ORGANIZATION REPORT NUMBER
CI07-0015

9. SPONSORING/MONITORING AGENCY NAME(S) AND ADDRESS(ES)
THE DEPARTMENT OF THE AIR FORCE
AFIT/ENEL, BLDG 16
2275 D STREET
WPAFB OH 45433

10. SPONSOR/MONITOR'S ACRONYM(S)

11. SPONSOR/MONITOR'S REPORT NUMBER(S)

12. DISTRIBUTION/AVAILABILITY STATEMENT
Unlimited distribution
In Accordance With AFI 35-205/AFIT Sup 1

13. SUPPLEMENTARY NOTES

14. ABSTRACT

15. SUBJECT TERMS

16. SECURITY CLASSIFICATION OF:			17. LIMITATION OF ABSTRACT	18. NUMBER OF PAGES	19a. NAME OF RESPONSIBLE PERSON
a. REPORT	b. ABSTRACT	c. THIS PAGE		27	19b. TELEPHONE NUMBER *(Include area code)*

Anatomical and Physiological Characteristics of the Ferret Lateral Rectus Muscle and Abducens Nucleus

Authors:

Keith N. Bishop[1], J. Ross McClung[1], Stephen J. Goldberg[1], Mary S. Shall[2]

K. N. Bishop[1], J. R. McClung[1], S.J. Goldberg[1]
Department of Anatomy and Neurobiology
Medical College of Virginia Campus
Virginia Commonwealth University
1101 E. Marshall St. PO Box 980709
Richmond, VA 23298-0709

Corresponding Author

M.S. Shall[2]
Department of Physical Therapy
Medical College of Virginia Campus
Virginia Commonwealth University
1200 East Broad St, PO Box 980224
Richmond, VA 23298-0224
e-mail: msshall@vcu.edu
Tel (804) 828-0234
Fax (804) 828-8111

Running Head: Lateral Rectus Motor Units in Ferret

Abstract

The ferret has become a popular model for neurodevelopmental and physiological research in the visual system. Accordingly, we studied single motor units in the ferret extraocular system. Using extracellular stimulation, 62 individual motor units in the ferret abducens nucleus were evaluated for their contractile characteristics. Of these motor units, 56 innervated the lateral rectus (LR) muscle alone while 6 were split between the LR and retractor bulbi (RB) muscle slips. In addition to individual motor units, the whole LR muscle was evaluated for twitch, tetanic peak force and fatigue. Current pulses of 0.2ms duration for twitch generation were followed by 150 ms tetanic trains ranging from 50 Hz to 220 Hz. The abducens nucleus was examined with CTHRP/TMB histochemistry and found to contain an average of 183 motoneurons. Samples of LR mid muscle belly were found to contain an average of 4687 fibers, indicating an LR innervation ratio of 25.6:1. The abducens nucleus motor units showed a twitch contraction time of 15.4 ms, a mean twitch tension of 30.2 mg, and an average fusion frequency of 154 Hz. Single unit fatigue index averaged .634. Whole muscle twitch contraction time was 16.7 ms with a mean twitch tension of 3.32 g. The average fatigue index of whole muscle was .408. Compared to cat and squirrel monkeys, the ferret LR motor units contract more slowly yet more powerfully. The functional visual requirements of the ferret may explain these fundamental differences.

Abstract

The ferret has become a popular model for neurodevelopmental and physiological research in the visual system. Accordingly, we studied single motor units in the ferret extraocular system. Using extracellular stimulation, 62 individual motor units in the ferret abducens nucleus were evaluated for their contractile characteristics. Of these motor units, 56 innervated the lateral rectus (LR) muscle alone while 6 were split between the LR and retractor bulbi (RB) muscle slips. In addition to individual motor units, the whole LR muscle was evaluated for twitch, tetanic peak force and fatigue. Current pulses of 0.2ms duration for twitch generation were followed by 150 ms tetanic trains ranging from 50 Hz to 220 Hz. The abducens nucleus was examined with CTHRP/TMB histochemistry and found to contain an average of 183 motoneurons. Samples of LR mid muscle belly were found to contain an average of 4687 fibers, indicating an LR innervation ratio of 25.6:1. The abducens nucleus motor units showed a twitch contraction time of 15.4 ms, a mean twitch tension of 30.2 mg, and an average fusion frequency of 154 Hz. Single unit fatigue index averaged .634. Whole muscle twitch contraction time was 16.7 ms with a mean twitch tension of 3.32 g. The average fatigue index of whole muscle was .408. Compared to cat and squirrel monkeys, the ferret LR motor units contract more slowly yet more powerfully. The functional visual requirements of the ferret may explain these fundamental differences.

Introduction

The eye must be capable of rapid and coordinated movements to allow the acquisition, fixation, and tracking of visual targets. It is the extraocular muscles (EOM) that move the globe in order to acquire and fixate visual targets. EOMs are unique skeletal muscles in terms of innervation and functional capabilities. Evaluation of the EOMs has determined that their speed of contraction far outpaces most skeletal muscles (6; 43). Lessons learned from hindlimb skeletal muscle regarding variable resistance due to changing joint position or movement occurring at the proximal or distal muscle insertion point do not apply to the EOM system because the recti extraocular eye muscles have only a single axis of movement, no variation of resistance, no extremity lever arm length changes, nor anti-gravity variations (39; 40). Rather, the EOM system is concerned with maintaining gaze control and the ability to acquire visual targets (36).

A great deal has been written on the physiology of EOM in animal models such as the cat and monkey (15; 24; 25; 31; 34). The evaluation of cat and monkey EOM motor units has revealed that these motoneurons can be classified into five functional categories based on twitch capabilities, fusion frequency, and fatigue (16; 43; 44; 46). While the EOM motor units in both these animals can be classified into similar groupings, each species display different contractile characteristics just as their functional visual demands also differ (16; 42-44; 46). For example, the cat LR motor units produce a twitch tension nearly three times stronger than that of the squirrel monkey while the monkey LR motor units are faster than the cat in both time to peak and fusion frequency (42; 43). Another potential difference between cat and Monkey LR motor units is the presence of nontwitch motor units (21; 34; 43). Nontwitch motor units have been identified in the cat but not in the squirrel monkey to date. The nontwitch motor unit propogates an action potential only when stimulated with tetanic trains

While contractile differences between species have been seen, another significant divergence between the studied species is that of predictive and linear summation of forces (16-18; 42). The cat hind limb whole muscle tensions have been shown by Burke to equal the predictive values from the summation of individual motor units (7). More recent evaluations of cat hind limb found that the actual whole muscle tension is greater than the predicted tension (10; 14; 37). Contrasted with hindlimb summation findings are EOMs that display whole muscle tensions that are only a fraction of the predicted values obtained from single unit data (16; 18). Specifically, the squirrel monkey actual LR whole muscle twitch force is only 5% of the predicted force whereas the cat actual LR whole muscle twitch force is 37% of the estimated value (16; 18). The loss of actual contraction tension might be due to the EOM muscle fibers branching into neighboring fibers while other fibers insert in a serial manner (28) or the possibility that motoneurons within the EOM motor nuclei maintain polyneuronal "safeguard" innervation patterns that result in redundant motoneuron cells. This polyneuronal innervation would make the algebraic calculation of predicted tensions artificially high (29). Regardless of the reason for the "lost" actual EOM

tension, the question remains as to why there is such a vast discrepancy between the cat and monkey using this force prediction method.

Because of the significant motor unit contractile differences seen between these animal models, we wanted to expand the understanding of extraocular functional parameters by undertaking a thorough evaluation of the ferret LR muscle and motor units within the abducens nucleus. Having actual LR contractile characteristics from the ferret, we can predict if the summation of forces follows the trend seen in other animals. The ferret has become an available and affordable model in neurodevelopmental and multi-sensory research. To our knowledge, a detailed evaluation of the extraocular system in the ferret has not been done.

Methods

Muscle Physiology

All procedures for the care and use of ferrets complied with the United States Public Health Service Policy on Humane Care and Use of Laboratory Animals. The Institutional Animal Care and Use Committee at Virginia Commonwealth University approved all experimental measures. All animals were obtained from Marshall Research Animals, (North Rose, NY).

Nine adult male ferrets (Mustela putorius furo) weighing between 1.35 – 2.1 kg were pre-anesthetized with an intramuscular injection of Robinul-V (.2 ml/kg), Ketamine (.2 ml/kg), and Xylazine (.02 ml/kg) prior to each experiment. Following pre-anesthesia, the animal was given Isoflurane at 3.0% via a small mask for several minutes to make certain of deep anesthesia. The topical anesthesia Cetacaine was sprayed into the oral pharynx prior to intubation. An intubation tube was introduced to allow Isoflurane to be continually administered throughout the duration of the experiment at a flow rate of 1.5-3.0% together with approximately 1.0 liter of oxygen per minute to keep the animal in a state of deep anesthesia (no withdrawal to paw pinch). The ferret was monitored at all times by way of a SurgiVet V9004 (Tulsa OK). A rectal probe continually recorded heart rate and oxygen saturation, while respiration rate and expiratory carbon dioxide were recorded through the intubation tube. Body temperature was maintained by a heating pad under the animal. To maintain hydration, the animal was injected subcutaneously with 5 ml of normal saline after 3 or 4 hours of experimental procedure and approximately every two hours thereafter.

With the ferret's head secured in a Kopf stereotaxic frame using the Kopf squirrel monkey adaptor (model 1248, Kopf Instruments, Tujunga, CA), a midline incision was made from the nasion to the upper cervical region. The temporalis muscle on the right side as well as portions of the masseter muscle was removed to expose the periorbital structures on the lateral side of the eye. Since the lateral bony orbit is incomplete in the ferret, care was taken to ensure the lateral rectus (LR) muscle was not damaged during the surgical procedure. The LR muscle was identified and a 5-0 silk suture passed behind and tied around the tendon at the point of insertion. This suture knot was secured with a drop of tissue glue prior to the tendon being released from the globe. As the LR tendon was being released from the globe, the underlying lateral retractor bulbi (RB) muscle slip was identified, separated from the global portion of the LR and left attached to the globe. The suture loop from the LR muscle was placed around a hook attached to a semiconductor force strain gauge (Pixie Model 8101, Endevco) adjusted to maintain correct anatomical alignment. This strain gauge has a natural frequency of 2 Khz and a compliance of 2 μm/g. The LR was kept moist through the periodic application of warm mineral oil. Additional suture loops were placed through the anterior surface of the globe and connected to a second strain gauge (ADInstruments MLT 050D, Colorado Springs, CO). The second strain gauge was positioned directly anterior to the eye to record tension generated by the RB muscles.

A single craniotomy was performed through the right posterior parietal bone for the introduction of two different electrodes. Through this craniotomy, a majority of the cerebellum was removed via suction to expose the floor of the fourth ventricle. A bipolar steel insulated electrode with 0.5 mm exposed tips was driven to the abducens nerve on the ipsilateral side (stereotaxic coordinates: Posterior 6.2; Lateral 2.9; and a variable depth depending on the size of the animal). Cranial Nerve VI was stimulated via the bipolar electrode and the LR strain gauge was optimally positioned for maximal isometric tension in the LR. The RB strain gauge was also optimally positioned in the same manner.

All stimulation paradigms were delivered by an A.M.P.I. Master-8 programmable pulse generator. Amplitude of the stimulation was regulated through a high voltage World Precision Instruments stimulus isolator (WPI Model A360, Sarasota FL).

Insulated electromyographic (EMG) wires (.002 in, 195 Ω/ft) were inserted through a 28-gauge needle into the substance of the LR muscle approximately 3 mm from the detached tendon in the distal muscle and the second wire through the proximal muscle belly. These EMG wires were connected to a BioAmp (ADInstruments) interface with the computer recording program Chart© (ADInstruments). The EMG was grounded with a silver wire through the contralateral temporalis muscle.

A tungsten electrode (10-15 μm, 5-10 MΩ) was introduced into the ipsilateral abducens nucleus. The ideal location for this tungsten electrode was determined by an antidromic field potential that was originated from the abducens nerve bipolar stimulating electrode and recorded via an ExCell3+ (FHC, Bowdoinham ME) preamplifier. Once a strong abducens nucleus field potential was identified, the same tungsten electrode was used for the extracellular stimulation of individual motoneurons. The tungsten microelectrode was driven by a Kopf hydraulic microdrive (Tujunga, CA) unit that recorded the exact depth of penetration.

When the tungsten electrode was driven close to a single motoneuron, the presence of the cell was confirmed by a small amplitude twitch stimulation that caused an all-or-nothing response by the motor unit that was detected from the strain gauge on a Tektronix 5111A oscilloscope (Tektronix, Inc., Beaverton OR) or through the appearance of an EMG signal. The stimulation amplitude and depth of electrode placement were adjusted to ensure only a single motor unit was activated. Each motor unit was evaluated by at least ten single twitch stimulations (1 Hz at 0.2 ms duration) followed by nine tetanizing trains of 150ms beginning at 50 Hz and increasing up to 220 Hz in increments of approximately 20 Hz. The twitch evaluation was performed prior to any tetanic stimulation in order to avoid potentiation. Each twitch stimulation pulse was delivered once per second and the tetanic stimulation trains were separated by five seconds to allow the muscle force to completely return to baseline. Following this stimulation paradigm, a fatigue protocol was performed that consisted of 75 Hz trains of 500ms duration per second for two full minutes. Occasionally while searching for motoneurons, a 50 Hz tetanic train was stimulated in an attempt to locate a distant motoneuron. These intermittent tetanic stimulations allowed the

possibility of locating a nontwitch motor unit. As many motor units as possible were evaluated from each animal. Following this individual motor unit testing on each animal, the same stimulation procedure was applied to the entire abducens nerve through the bipolar electrode to evaluate whole muscle twitch tension, tetanic forces and fatigue.

Each force generated by either the LR or RB was recorded through the transducers to the Chart© program for later evaluation. The recorded twitches were analyzed for time to peak, overall maximal tension and half-relaxation time for ten separate twitch recordings per motor unit. The LR twitch contractions were averaged from 10 separate contractions to determine the contractile characteristics for each motor unit. The tetanic contractions were evaluated for peak force. Individual tetanic trains were evaluated to determine the specific frequency that produced a characteristic fused tension. No effort was made to quantify the amount of tension from the four RB slips still attached to the globe. The recording of RB activity was only used to document if RB contraction occurred from the stimulation of the motoneuron. The fatigue index (FI) was determined using the Burke method as a ratio from the tension from the last of the fatigue stimulations to the tension from the first fatigue stimulation. The higher the FI, the more the motor unit is able to exert sustained tension throughout the fatiguing stimulation protocol.

Descriptive statistics were calculated for each contractile parameter including twitch tension, maximum tetanic tension, twitch contraction time, twitch half relaxation time, and fatigue index. An unpaired student t-test was performed to determine significance between motor unit groupings at various stimulation frequencies.

Anatomical Evaluation

In a separate series of experiments, three adult male ferrets (1.4 – 1.75 kg) were used for anatomical study of the LR muscle as well as histological evaluation of the abducens nucleus.

The ferret was anesthetized as described previously while maintaining a patent airway and being monitored for distress. While in this state, the lateral edge of the skin surrounding the right eye was carefully cut and the underlying connective tissue painstakingly dissected to reveal the LR tendon as it inserts on the globe. After carefully exposing this tendon a small probe was passed under the muscle and pulled slightly forward to expose the LR muscle belly. A Hamilton micro-injection 22 gauge needle was inserted approximately 1cm into the LR muscle belly maintaining the correct parallel alignment to the muscle. At this depth a bolus of approximately 25-40 μl of horseradish peroxidase conjugated with the subunit B of cholera toxin (CTHRP) was injected. An additional 10-25 μl (50 μl total) was injected in the muscle along the needle track in areas closer to the distal tendon but still within the muscle belly. Following the CTHRP injection, gentle pressure was applied to the outer orbital edge of the muscle in an effort to prevent overflow of the CTHRP into other periorbital structures. The lateral eye connective tissue and skin was carefully sutured. Topical Xylocaine was applied to the surgical site. Following this procedure, the

Isoflurane was discontinued and the animal was monitored closely as it regained consciousness. As the animal became more alert it was given water by mouth and returned to the animal care facility 1-2 hours after the surgery. Twenty-four hours after the CTHRP injection, the animal was perfused transcardially with a phosphate-buffered mixture of 1% paraformaldhyde and 1.25% glutaraldhyde over a one hour period. Bilateral LR muscles were removed and frozen in embedding medium at -80° C. Following perfusion, the brainstem was removed and immersed in fixative for 8 hours.

The brainstem was blocked and stored an additional 2 hours in phosphate buffer. The blocked section was serially sectioned with a vibratome into 50 μm, transverse sections. At this point the sections were processed for HRP neurohistochemistry according to the modified Mesulam technique with tetramethylbenzidine (TMB) as the chromogen. Following the TMB incubation protocol, the sections are rinsed in distilled water and then mounted on glass slides. After 24-48 hours of dehydration, the sections were counterstained with neutral red and cover slipped with permount. The evaluation of the brainstem sections was conducted using the Image-Pro digital imaging software and an Olympus BH-2 microscope with an attached CoolSNAP-Pro digital camera (Media Cybernetics, Silver Spring MD). Each section was analyzed for the presence of dark HRP reaction product in the motoneurons by focusing the microscope on the top of the slide and slowly focusing through the 50 μm section ensuring that each cell is identified and counted. By evaluating the top and bottom of each section as well as sequential sections, it was possible to ensure that any cell bodies that were cut and thus seen on multiple sections were only counted once.

The non-injected and non-stimulated muscles were harvested and stored at -80° C until the time they were sectioned into 10 μm sections with a cryostat and mounted on glass slides. Muscle specimens were stained with H & E and then cover slipped with permount. The evaluation of three midbelly sections from each muscle specimen was conducted using the same imaging system as the brainstem sections. Individual muscle fibers were counted using Image-Pro software (MediaCybernetics, Silver Spring, MD) that allows a marker to be placed on each muscle fiber in the digital image.

Anatomical data also had descriptive statistics for average number of muscle fibers and motoneurons. For each sample of LR muscle an average of three midsubstance sections was counted. An unpaired student t-test was performed to determine significance between muscle fiber diameters in the global vs. orbital layers.

Results
The results are expressed as mean $\pm$ standard deviation unless otherwise noted. Statistical significance was set at $p \leq 0.05$.

Motor-unit contractile characteristics

The extracellular stimulation of individual motoneurons via tungsten electrode within the ferret abducens nucleus resulted in the contraction of either pure LR or split LR-RB muscle units. Of the 62 total motoneurons with a complete physiological evaluation, fifty six innervated only LR muscle units. The remaining 6 motor units (9.7%) had a split innervation between RB and LR. This percentage of split motor units in the ferret is comparable to that seen in the cat (12; 19).

Each of the motor units responded to a single electrical pulse as well as tetanic stimulation (Fig 1A). The individual motor units in this study were located and initially evaluated using single pulses which limited the possibility of locating nontwitch motor units as described in previous works (43). The LR motor units (n = 56) had an average twitch tension of 30.2 $\pm$ 18.5 mg, (range 6.7 – 104 mg) and an average twitch time to peak contraction time of 15.4 $\pm$ 5.79 ms, (range 6.8 – 28 ms). Motor units with LR -RB split innervation (n = 6) had an average LR portion twitch tension of 27.8 $\pm$ 11.0 mg, (range 17.3 – 42.9 mg) and an average LR portion time to peak contraction time of 23.7 $\pm$ 4.4 ms, (range 17.9 – 29.5 ms).

Tetanizing stimulations to the LR isolated motoneurons displayed a maximal force of 327 $\pm$ 334 mg (range 36 – 1530 mg). The LR-RB motor units had an average maximal LR component tetanic tension of 523 $\pm$ 271 mg (range 153 – 790 mg). Figure 2 illustrates the wide distribution of tetanic contraction characteristics for the LR only units as well as the LR-RB motor units. Eighty eight percent of the units evaluated achieved maximal tension at or above the fusion frequency. During unfused tetanic stimulation, there was no evidence of “sag” seen in any of the motor unit or whole muscle contractions (8). On two occasions, a nontwitch motor unit was identified from an isolated 50 Hz tetanic train. These two nontwitch motor units responded well to the variable frequency stimulation protocol but the fatigue test was inconclusive. The average tetanic tension from these two nontwitch units was 39.5 mg (22 – 63 mg). Both units achieved its maximal tension at frequencies below 140 Hz.

The fusion frequencies of the LR motor units varied between 120 and 220 Hz with a mean frequency of 154.6 $\pm$ 20.7 Hz. To categorize the LR motor units into either fast or slow groupings, those motor units with a fusion frequency below the population mean are considered “slow” and those with a fusion frequency above the population mean are considered ”fast” (16; 43; 46). All six of the LR-RB units had a fusion frequency at 140 Hz or below. In an effort to determine if using the fusion frequency as a way of organizing the LR motor units into groupings of fast or slow actually realized true differences, a force tension (F-T) curve was created for each frequency normalized against the highest

frequency (220 Hz). The contractile differences between the groups were seen at each frequency as a percentage of the tension created at maximal frequency (Fig 3). The fast units required a significantly higher stimulation frequency to achieve the comparable tension developed by the slow units at lower frequencies. Using an un-paired t-test, a significant difference was seen between stimulated tension of the slow and fast units at 120 Hz ($p = 0.013$), 140 Hz ($p = 0.017$), 160 Hz ($p = 0.034$), and 180 Hz ($p = 0.038$).

A 2-minute fatigue test was performed on each motor unit. The LR only motor units had a mean fatigue index (FI) of 0.63 ± 0.39 (range 0.09 – 2.4). The mean FI for the LR-RB motor units was 0.72 ± 0.18 (range 0.54 – 1.0) (Fig 1B). The LR units with a FI above the mean were classified as fatigue resistant and those below the mean were categorized as fatigable. Twenty-two motor units maintained >0.63 of initial tension following fatigue testing while 34 motor units lost enough tension during 2 minutes of stimulation to drop <0.63 from beginning to end of the testing.

Combining the fusion frequency and fatigue allowed the further classification into four groups (43). These groups were Slow fatigue-resistant, SR ($n = 6$), Slow fatigable, SF ($n = 15$), Fast fatigue-resistant, FR ($n = 16$), and Fast fatigable, FF ($n = 19$). Table 1 summarizes the specific contractile characteristics for the four categories above as well as the LR-RB units left together as one group.

Whole Muscle Contractile Characteristics

Following the evaluation of single motor units, the abducens nerve received supramaximal stimulation through the bipolar electrode. The average LR whole muscle twitch tension was 3.31 ± 1.29 g (range 1.58 – 5.32) with an average time to peak contraction time of 16.7 ± 6.6 ms (range 10.2 – 27.4 ms). The average maximal tetanic tension was 17.05 ± 7.7 g (range 8.9 – 34.9 g) with an average fusion frequency of 144 ± 13.3 Hz. The average fatigue index for the whole LR muscle was 0.408 ± 0.252 (range 0.03 - 0.747). Figure 4A displays an example of whole muscle twitch and various tetanic contractions while Fig 4B illustrates whole muscle fatigue testing.

Anatomical Evaluation

This anatomical study was conducted to gain an accurate understanding of the number of motoneurons within the ferret abducens nucleus and the number of muscle fibers that make up the LR. The histochemical evaluation of the abducens revealed that an average of 183 ± 27 (SD) motoneurons are loosely packed ventral to the facial colliculus (Fig 5). The mean cell diameter is $27.1 \pm 4.3\ \mu m$ (SD) (range 21.2 – 44.2 μm). An average of 12.7 brainstem sections contained reacted motoneuron cells. Using the 50 μm thickness of each section, the average rostral to caudal nucleus pool length is 650 μm. An accessory abducens nucleus was seen ventrolateral to the primary abducens nucleus in one animal indicating an overflow of CTHRP into one or more RB muscle slips.

Turning attention to the LR muscle fibers, it was determined that an average of 4687 $\pm$ 707 fibers are contained in the mid belly muscle (Fig 6). No effort was made to conclude the specific number of fibers isolated in the global or orbital layers. The size of fibers was evaluated from each layer with the inner global layer fibers having an average diameter of 18.35 $\pm$ 3.5 μm. The outer orbital layer contained muscle fibers with the significantly smaller average diameter of 11.76 $\pm$ 2.4 μm. Having both the number of motoneurons present in the primary abducens nucleus as well as the total number of LR muscle fibers, the ferret LR innervation ratio is 25.6:1.

Discussion

The major findings regarding ferret lateral rectus motor units were that: 1) the use of fusion frequency enabled the population of evaluated motor units to be classified into fast and slow, 2) further classification using fatigue criteria resulted in the categories of FF, FR, SF, and SR, 3) nontwitch motor units are found in the ferret, 4) whole muscle forces evoked by VIth nerve stimulation were lower than predicted by either twitch or tetanic contraction average force multiplied by the number of motoneurons found within the abducens nucleus.

Motor-unit contractile characteristics

Clamann stated it well when he reported that “the muscles that move the eye are a world unto themselves”(9). In comparing the EOMs to limb muscles, the fast contractile speed of eye muscles as well as a low innervation ratio that aids in the precision of controlled movement to provide clear binocular vision have been noted (3; 4; 9; 11; 41; 47).

The ferret lateral rectus motor units were classified according to their twitch capabilities, fusion frequency, and fatigue index. Using the F-T curve clearly demonstrates that the slow units are a unique group that achieve maximal tension at notably lower frequencies than the fast units. However fast and slow groupings did not produce significantly different tensions with the very lowest frequencies. The significant difference between these groups is seen in the frequency range of 120 – 180 Hz. Any differences between these groups are again lost at the frequencies at or above 200 Hz. At these higher frequencies the slow motor units are past their ideal fusion frequency and have already achieved their maximal tension. Above their ideal fusion frequency, the slow units are declining in tension whereas the fast units are reaching the ideal frequencies for them to achieve maximal tension. These different physiological reactions by fast and slow units to variable stimulation frequencies has also been seen in cat and human single unit evaluations (5; 48). The F-T curve (Fig 3) also shows that the 75 Hz fatigue test used in this study was ideal in the ferret since no significant difference was seen between the motor unit groupings at that frequency (45). The 75 Hz fatigue testing frequency was well below the average fusion frequency thus preventing excessive stress on the motor unit. This normalized F-T curve method of ensuring motor unit grouping differences has not been previously utilized in the EOM system.

The twitch type motor units responded to single pulse stimulation that allowed the categorization of twitch tension and then tetanic tension while progressing through the tetanic train stimulation paradigm. The average ferret single motor unit twitch tension was very comparable to that seen previously in the cat but three times larger than the squirrel monkey (15; 16; 18; 31; 42; 43; 46). In comparing LR time to peak twitch contraction time, the cat is two times and the monkey three times faster than the ferret. The fusion frequency in the ferret was much lower than both animals. In terms of tetanic contractions, the average tetanic tension produced in the ferret LR is much larger than both the cat and squirrel monkey (16-18; 42; 43). While the method used in this study to

locate motoneurons severely limited the likelihood of locating nontwitch motor units, two such units were identified which confirms their presence in the ferret.

The specific motor unit group characteristics outlined in table 1 indicate that the Fast Fatigable motor unit group had the fastest time to peak, highest fusion frequency, and largest twitch tension, corresponding to that previously seen in the cat LR (43). The ferret Slow Resistant motor unit group is surprising in that the average twitch tension is not the small fraction of the tension produced by the Fast Fatigable group as seen in the cat. The tetanic tension generated from the ferret LR Slow Resistant group is larger than the typically powerful Fast Fatigable motor units in the cat.

Whole Muscle Contractile Characteristics

While the ferret had comparable single motor unit twitch averages with that of the cat, the whole muscle results were drastically different. The ferret whole muscle twitch ($\bar{x}$ = 3.3 g) and tetanic forces are more similar to the squirrel monkey than to the cat (16). The average cat LR maximal tetanic contraction ($\bar{x}$ = 109 g) is 6.5 times greater than either the ferret ($\bar{x}$ = 17 g) or squirrel monkey ($\bar{x}$ = 13.7 g) (16; 43). Such a large disparity in whole muscle contractile capabilities between the cat and ferret LR muscles must be addressed in terms of a functional difference. The cat and ferret are both carnivore hunters but with completely differing hunting styles. When hunting, the cat will visually scan a wide area watching for any potential prey to expose itself. Noticing a possible prey, the cat will fixate its visual attention on the prey as it begins to inch closer for an attempted capture (20; 35). The hunting cat relies on visual input more than olfaction such as is seen in the dog and ferret. The benefits of a fast eye control system can be appreciated in the cat hunting style. In contrast to the cat, the ferret is a far sighted nocturnal hunter that never stays still but is quickly exploring its environment with rapid up and down head movements (20; 26; 32). Vision does not seem to be a primary tool for ferret behavioral testing in that visual stimuli do not always attract the ferret's attention(38). When a ferret does become interested, its visual system is best able to follow objects moving at speeds of 25 – 45 cm/sec which is approximately the speed of mice (2). Once the ferret has become interested in a potential prey, olfaction appears to become more important than vision in the hunting behavior (2). As the ferret explores the darkened environment of borrows, the need for rapid nystagmus control is reduced. The ferret eyes are more laterally placed than either cats or monkeys which increases the visual field to 270° compared to 180° for cats (32). In addition to having the eyes in a more lateral position, the ferret pupil is a horizontal slit coupled with a horizontal retinal visual streak extending nasally from the area centralis, suggesting a visual horizontal bias that might reduce the amount of required functional lateral globe movement (32). In this scenario, the slower contracting muscle units with pronounced endurance (SR) would be the most beneficial units to control the whole muscle function.

Predicted muscle tension

We have previously evaluated the actual lateral rectus tensions produced via stimulation of the VIth nerve and found these forces to fall below the predicted values from multiplying the average single motor unit forces by the number of known motoneurons (13; 16; 18; 43). In the ferret, the average single LR motor units twitch force (30.2 mg) multiplied by the number of known motoneurons (n = 183) *should* produce a whole muscle twitch tension of 5.5g while the actual value (3.3 g) is only 60% of the predicted. Actual ferret LR maximal tetanic tension produced only 28% of the predicted force (17 g actual vs. 60 g predicted). The "loss" of actual LR tension is even more drastic in the monkey in that the actual twitch tension is only 5% of the predicted value and the maximal tetanic tension is only 3.7% of estimated values(16).

The reasoning behind this lost muscle force remains unclear. Extraocular muscle fiber serial arrangement and branching has often been postulated (1; 18; 23; 27). The impact of this muscle architecture may result in tension being lost during whole nerve stimulation because the tension generated within one muscle unit can not be completely transferred to intramuscular connective tissue because the adjoining muscle fibers are also contracting during the whole nerve stimulation (18). When adjacent and connected muscle fibers are each contracting, an aspect of antagonism might occur that dampens the total generated force.

In addition to force dispersal, another potential source for the non-algebraic summation of EOM motor units is that of polyneuronal innervation (22; 29; 30). Having multiple motoneurons innervating individual muscle fibers might suggest that more motoneurons exist than are needed for the basic function of the EOM (29). Having "extra" motoneurons would give an explanation as to why the simple algebraic prediction of whole muscle forces is drastically over estimated in the EOM. The possibility that EOM might in part be polyneuronally innervated may support the notion why this motor system protects the function of eye muscles during some motoneuron wasting diseases (29; 33).

The findings in the study imply that the physiological characteristics of EOM motor units vary depending on the functional requirements of the animal under investigation. The cat has fast LR contractile characteristics and a low LR innervation ratio that aids with absolute ocular precision. Contrast that animal that relies heavily on vision in hunting with the ferret that maintains much slower LR motor units and a large innervation ratio that might be representative of the ferret's lack of visual dependence with hunting tasks. An evolutionary advancement from ferret up to cat and finally squirrel monkey has been identified with significant differences in ocular control provided by motor units that provide fine visual precision and safeguards against disease.

Reference List

1. **Alvardo-Mallart R and Pincon-Raymond M**. Nerve endings on the intramuscular tendons of cat extraocular muscles. *Neurosci Lett* 2: 121-125, 1976.

2. **Apfelbach R and Wester U**. Quantitative Effect of Visual and Tactile Stimuli on Prey-Catching Behavior of Ferrets (Putorius-Furo L). *Behavioural Processes* 2: 187-200, 1977.

3. **Barmack NH**. Recruitment and suprathreshold frequency modulation of single extraocular muscle fibers in the rabbit. *J Neurophysiol* 40: 779-790, 1977.

4. **Barmack NH, Bell CC and Rence BG**. Tension and rate of tension development during isometric responses of extraocular muscle. *J Neurophysiol* 34: 1072-1079, 1971.

5. **Botterman BR, Iwamoto GA and Gonyea WJ**. Gradation of isometric tension by different activation rates in motor units of cat flexor carpi radialis muscle. *J Neurophysiol* 56: 494-506, 1986.

6. **Burke RE**. Motor unit types of cat triceps surae muscle. *J Physiol* 193: 141-160, 1967.

7. **Burke RE, Levine DN, Tsairis P and Zajac FE, III**. Physiological types and histochemical profiles in motor units of the cat gastrocnemius. *J Physiol* 234: 723-748, 1973.

8. **Burke RE, Levine DN and Zajac FE, III**. Mammalian motor units: physiological-histochemical correlation in three types in cat gastrocnemius. *Science* 174: 709-712, 1971.

9. **Clamann HP**. Motor unit recruitment and the gradation of muscle force. *Phys Ther* 73: 830-843, 1993.

10. **Clamann HP and Schelhorn TB**. Nonlinear force addition of newly recruited motor units in the cat hindlimb. *Muscle Nerve* 11: 1079-1089, 1988.

11. **Close RI and Luff AR**. Dynamic Properties of Inferior Rectus Muscle of the rat. *J Physiol* 236: 259-270, 1974.

12. **Crandall WF, Goldberg SJ, Wilson JS and McClung JR**. Muscle units divided among retractor bulbi muscle slips and between the lateral rectus and retractor bulbi muscles in cat. *Exp Neurol* 71: 251-260, 1981.

13. **Demieville HN and Partridge LD**. Probability of peripheral interaction between motor units and implications for motor control. *Am J Physiol* 238: R119-R137, 1980.

14. **Emonet-Denand F, Laporte Y and Proske U**. Summation of tension in motor units of the soleus muscle of the cat. *Neurosci Lett* 116: 112-117, 1990.

15. **Goldberg SJ, Lennerstrand G and Hull CD**. Motor unit responses in the lateral rectus muscle of the cat: intracellular current injection of abducens nucleus neurons. *Acta Physiol Scand* 96: 58-63, 1976.

16. **Goldberg SJ, Meredith MA and Shall MS**. Extraocular motor unit and whole-muscle responses in the lateral rectus muscle of the squirrel monkey. *J Neurosci* 18: 10629-10639, 1998.

17. **Goldberg SJ and Shall MS**. Lateral rectus whole muscle and motor unit contractile measures with the extraocular muscles intact. *J Neurosci Methods* 78: 47-50, 1997.

18. **Goldberg SJ, Wilson KE and Shall MS**. Summation of extraocular motor unit tensions in the lateral rectus muscle of the cat. *Muscle Nerve* 20: 1229-1235, 1997.

19. **Gurahian SM and Goldberg SJ**. Fatigue of lateral rectus and retractor bulbi motor units in cat. *Brain Res* 415: 281-292, 1987.

20. **Hein A, Courjon JH, Flandrin JM and Arzi M**. Optokinetic nystagmus in the ferret: including selected comparisons with the cat. *Exp Brain Res* 79: 623-632, 1990.

21. **HESS A and PILAR G**. SLOW FIBRES IN THE EXTRAOCULAR MUSCLES OF THE CAT. *J Physiol* 169: 780-798, 1963.

22. **Jacoby J, Chiarandini DJ and Stefani E**. Electrical properties and innervation of fibers in the orbital layer of rat extraocular muscles. *J Neurophysiol* 61: 116-125, 1989.

23. **Katz B**. The relation between force and speed in muscular contraction. *J Physiol* 96: 45-64, 1939.

24. **Lennerstrand G**. Fast and slow units in extrinsic eye muscles of cat. *Acta Physiol Scand* 86: 286-288, 1972.

25. **Lennerstrand G**. Mechanical studies on the retractor bulbi muscle and its motor units in the cat. *J Physiol* 236: 43-55, 1974.

26. **Lode T**. Activity Pattern of Polecats Mustela-Putorius I in Relation to Food-Habits and Prey Activity. *Ethology* 100: 295-308, 1995.

27. **Mayr R**. Structure and Distribution of Fibre Types in the External Eye Muscles of the Rat. *Tissue Cell* 3: 433-462, 1971.

28. **Mayr R, Gottschall J, Gruber H and Neuhuber W**. Internal structure of cat extraocular muscle. *Anat Embryol (Berl)* 148: 25-34, 1975.

29. **McClung JR, Cullen KE, Shall MS, Dimitrova DM and Goldberg SJ**. Effects of electrode penetrations into the abducens nucleus of the monkey: eye movement recordings and histopathological evaluation of the nuclei and lateral rectus muscles. *Exp Brain Res* 158: 180-188, 2004.

30. **McClung JR, Shall MS and Goldberg SJ**. Motoneurons of the lateral and medial rectus extraocular muscles in squirrel monkey and cat. *Cells Tissues Organs* 168: 220-227, 2001.

31. **Meredith MA and Goldberg SJ**. Contractile differences between muscle units in the medial rectus and lateral rectus muscles in the cat. *J Neurophysiol* 56: 50-62, 1986.

32. **Miller PE**. Ferret ophthalmology. *Seminars in Avian and Exotic Pet Medicine* 6: 146-151, 1997.

33. **Mosier DR, Siklos L and Appel SH**. Resistance of extraocular motoneuron terminals to effects of amyotrophic lateral sclerosis sera. *Neurology* 54: 252-255, 2000.

34. **Nelson JS, Goldberg SJ and McClung JR**. Motoneuron electrophysiological and muscle contractile properties of superior oblique motor units in cat. *J Neurophysiol* 55: 715-726, 1986.

35. **Pellis SM, Obrien DP, Wolgin DL, Kennedy S, Pellis VC and Teitelbaum P**. Escalation of Feline Predation Along A Gradient from Avoidance Through Play to Killing. *Behavioral Neuroscience* 102: 760-777, 1988.

36. **Porter JD, Baker RS, Ragusa RJ and Brueckner JK**. Extraocular muscles: basic and clinical aspects of structure and function. *Surv Ophthalmol* 39: 451-484, 1995.

37. **Powers RK and Binder MD**. Summation of motor unit tensions in the tibialis posterior muscle of the cat under isometric and nonisometric conditions. *J Neurophysiol* 66: 1838-1846, 1991.

38. **Rabe A, Haddad R and Dumas R**. Behavior and Neuro-Behavioral Teratology Using the Ferret. *Laboratory Animal Science* 35: 256-267, 1985.

39. **Robinson DA**. Is the oculomotor system a cartoon of motor control? *Prog Brain Res* 64: 411-417, 1986.

40. **Ruff RL**. More than meets the eye: extraocular muscle is very distinct from extremity skeletal muscle. *Muscle Nerve* 25: 311-313, 2002.

41. **Scott AB and Collins CC**. Division of labor in human extraocular muscle. *Arch Ophthalmol* 90: 319-322, 1973.

42. **Shall MS, Dimitrova DM and Goldberg SJ**. Extraocular motor unit and whole-muscle contractile properties in the squirrel monkey. Summation of forces and fiber morphology. *Exp Brain Res* 151: 338-345, 2003.

43. **Shall MS and Goldberg SJ**. Extraocular motor units: type classification and motoneuron stimulation frequency-muscle unit force relationships. *Brain Res* 587: 291-300, 1992.

44. **Shall MS and Goldberg SJ**. Lateral rectus EMG and contractile responses elicited by cat abducens motoneurons. *Muscle Nerve* 18: 948-955, 1995.

45. **Shall MS, Van Cleave S, Dimitrova DM and Goldberg SJ**. Lateral rectus muscle changes after bilateral neonatal labyrinthectomy in the ferret. *J Vestib Res* 15: 243-251, 2005.

46. **Shall MS, Wilson KE and Goldberg SJ**. Extraocular motoneuron stimulation frequency effects on motor unit tension in cat. *Acta Anat (Basel)* 157: 217-225, 1996.

47. **Spencer RF and Porter JD**. Biological organization of the extraocular muscles. *Prog Brain Res* 151: 43-80, 2005.

48. **Thomas CK, Bigland-Richie B and Johansson RS**. Force-frequency relationships of human thenar motor units. *J Neurophysiol* 65: 1509-1516, 1991.

A.

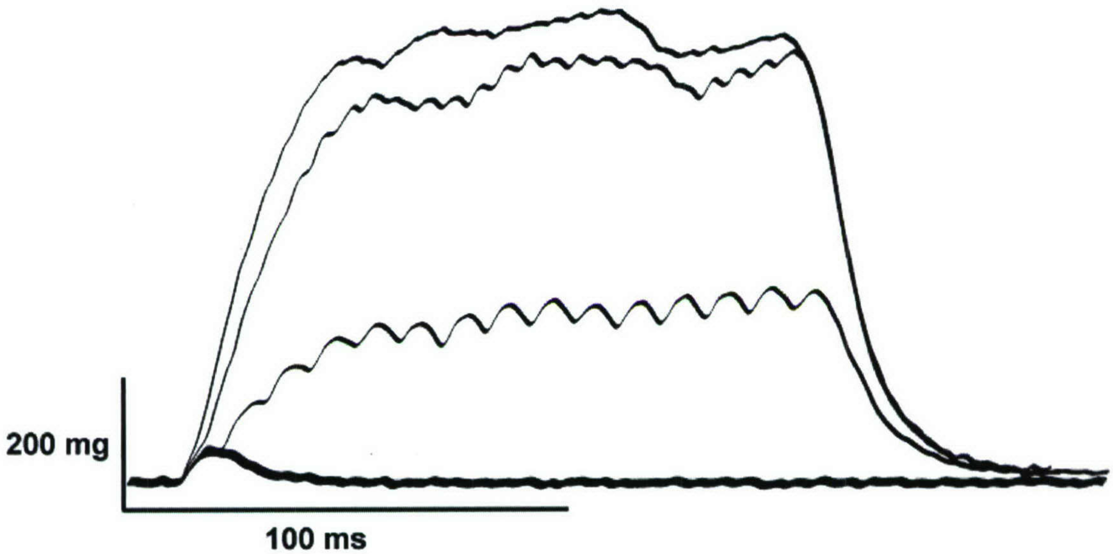

B.

Figure 1. Mechanical properties of a single LR motor unit. A. Lowest to highest tracings are twitch (57 mg), 75 Hz (333 mg), 160 Hz (652 mg), 220 Hz (733 mg). B. Fatigue testing of a single motor unit. The top tracing is the first tetanic response (177 mg) and the bottom trace is the 120th response after 2 minutes (22 mg). The fatigue index for this unit is .124.

A.

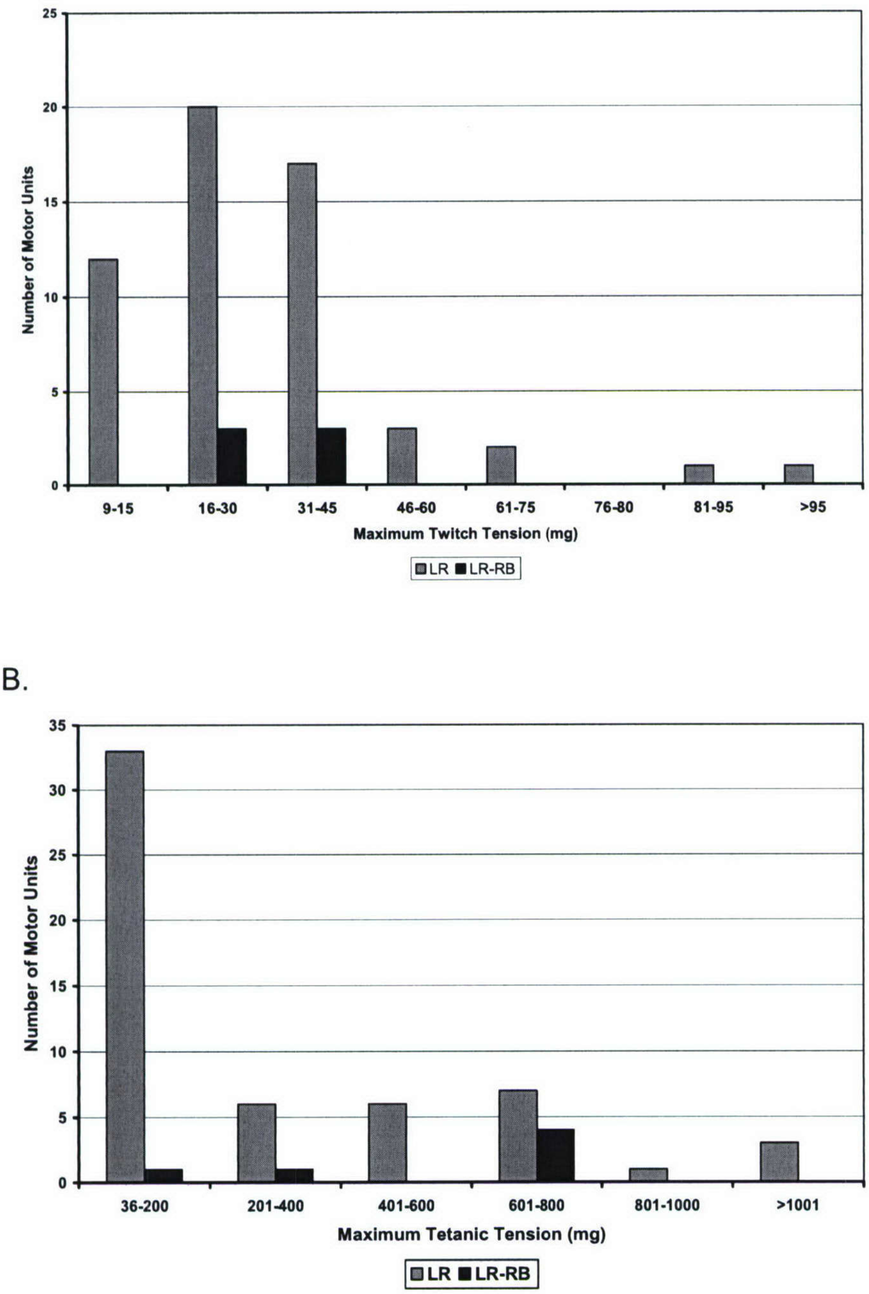

B.

Figure 2. A. Twitch tension for 56 LR units and 6 LR-RB units. B. Maximum tetanic tension for 56 LR motor units as well as 6 LR-RB motor units.

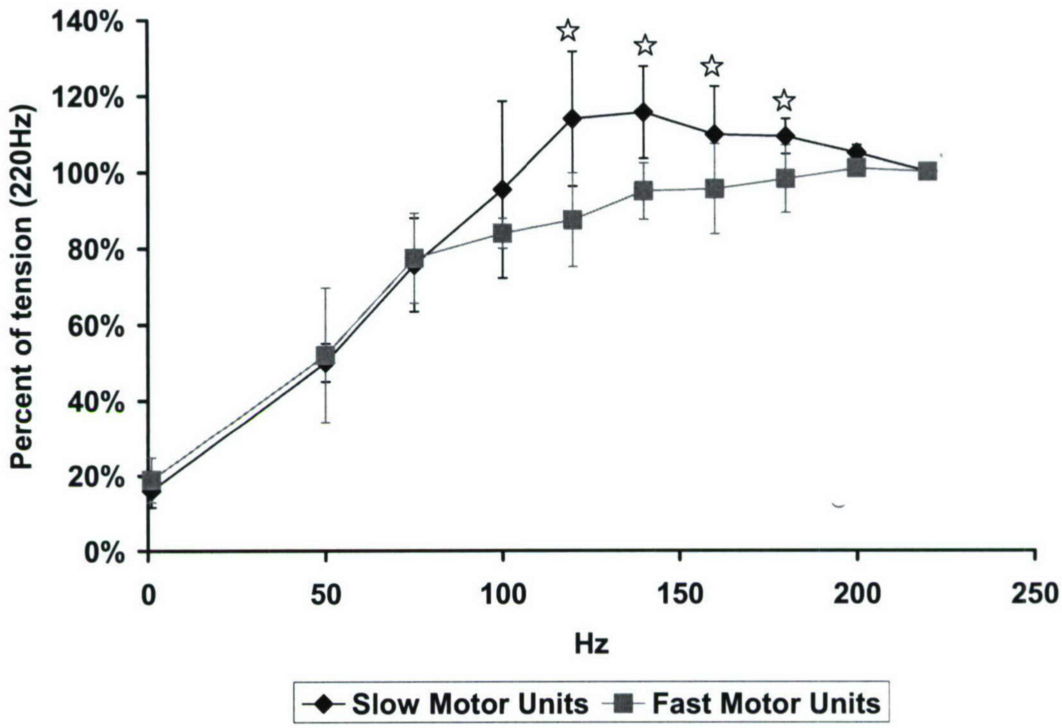

Figure 3. Normalized contractile characteristics for “fast” and “slow” motor units at each stimulation frequency compared to the highest frequency (220 Hz). Significance (*) is set at $p \leq 0.05$.

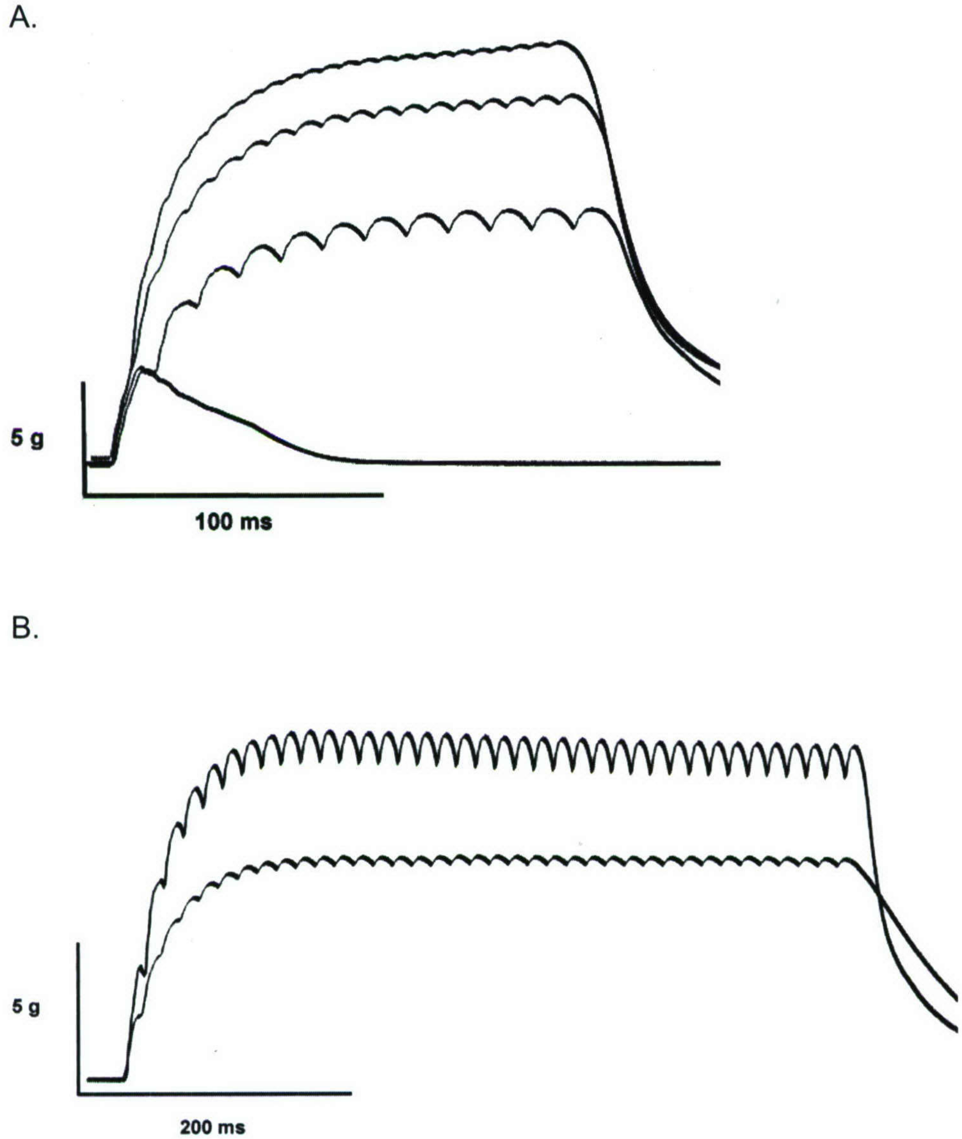

Figure 4. Contractile properties of lateral rectus muscle from supramaximal stimulation of abducens nerve. **A**. Lowest to highest tracings are twitch (4.3 g), 75 Hz (12.1 g), 160 Hz (17.1 g), 220 Hz (18.6 g). **B**. Fatigue testing of whole LR muscle. The top tracing is the first tetanic response (16.4 g) and the bottom trace is the 120th response after two minutes (10.7 g). The fatigue index for this muscle is.65.

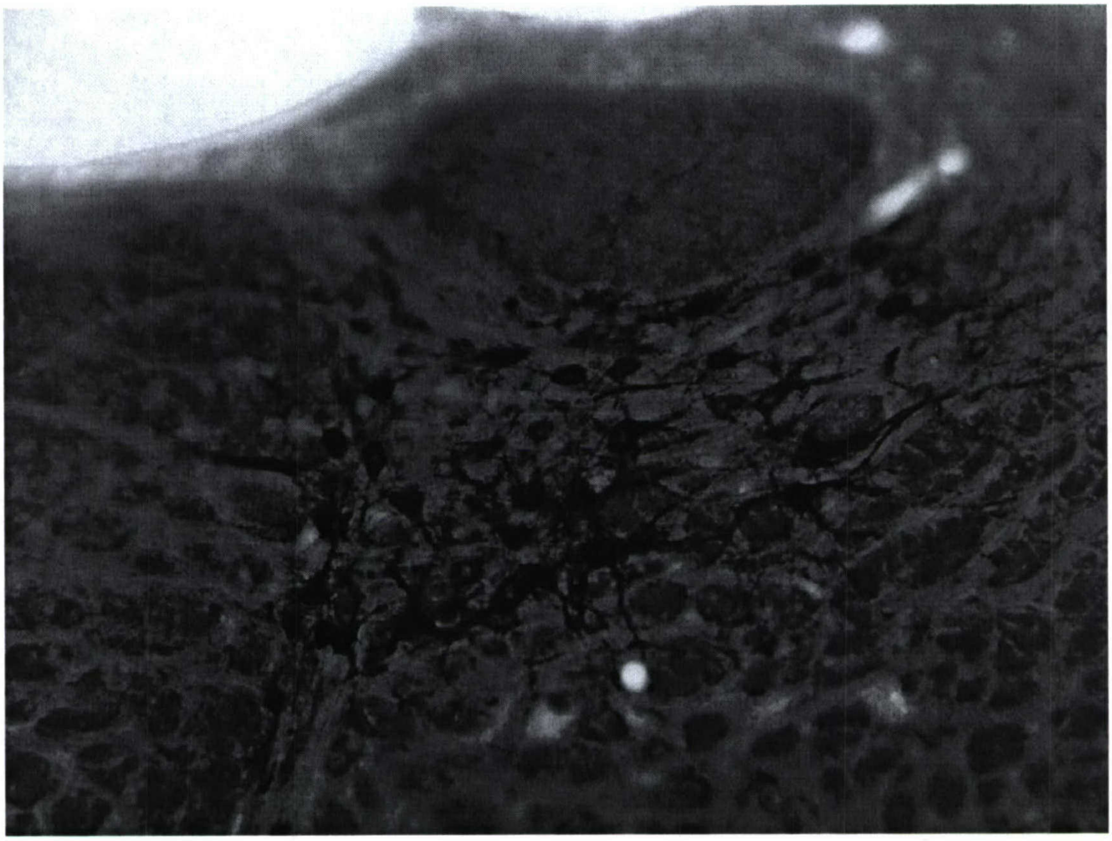

Figure 5. Photomicrograph of abducens nucleus with HRP reacted motoneurons.

A.

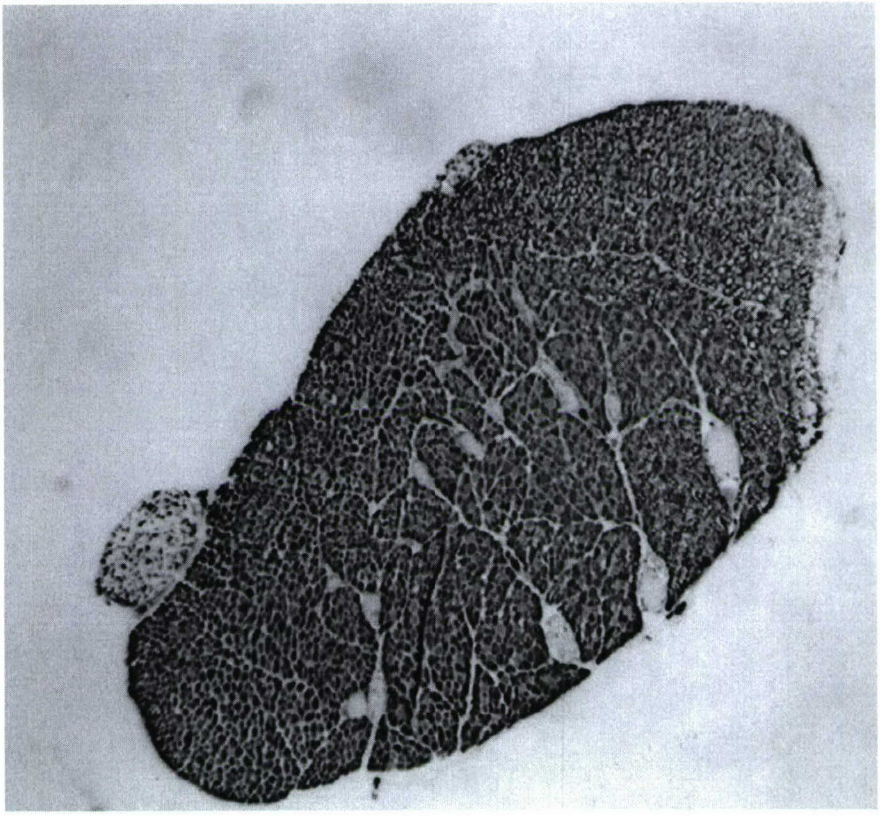

B.

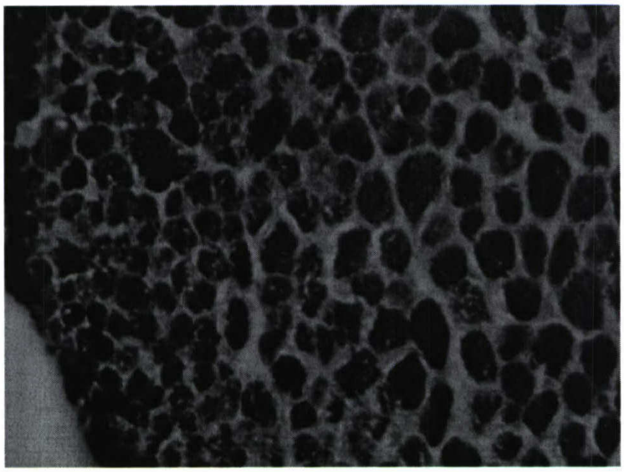

Figure 6. H & E histology of the lateral rectus. **A**. Whole muscle section. **B**. 40X magnification of the portion outlined. Note the smaller orbital fiber diameter on the left side of enlarged figure.

TABLE 1

Single Motor Unit Characteristics for Functional Categories

Characteristic	SR	SF	FR	FF	LR-RB
N	6	15	16	19	6
Fatigue Index	0.775	0.489	1.07	0.351	0.726
Fusion Frequency	127 Hz	135 Hz	166 Hz	169 Hz	137 Hz
Twitch Tension					
Mean (mg)	33.1	26.9	25.3	36.1	27.9
SD (mg)	8.3	9.6	10.2	28.1	11.0
TTP (ms)	20.6	17.5	14.7	12.6	23.6
Minimum (mg)	26.1	6.7	11.8	9.6	17.3
Maximum (mg)	46.8	39.6	43.9	104	50.6
Tetanic Tension					
Mean (mg)	473	311	172	426	523
SD (mg)	290	238	160	461	270
Minimum (mg)	84	67.0	36.0	84.0	153
Maximum (mg)	827	714	749	1530	790